INTERACTION OF A SHOCK WITH BLUNT BODIES STREAMLINED BY A SUPERSONIC STREAM

Yu. F. Makovskii and F. V. Shugaev

UDC 533.6.011.72

The density field is determined experimentally for plane shock incidence on blunt bodies streamlined by a supersonic gas stream.

Plane shock incidence on blunt bodies (cylinders with a flat or spherical nose) around which a steady supersonic gas stream flows is examined. . Such a problem arises in studying the effect of an explosion wave on a body flying at supersonic velocity in the atmosphere. There are computations of such an interaction in [1-3]. However, the accuracy of the numerical schemes used is not adequate to obtain information about the motion of the transient wave and the change in the gas parameters in the shock layer. Experimental data on the motion of the transient wave, the contact surface, and the pressure change at the body stagnation point are given in [4-6].

We investigated the gas density distribution near the body at various times. The experiments were performed in a two-diaphragm shock tube of 40 × 61 mm section. The model was placed in the working section. Two shocks were obtained in the tests, where the stream behind the first produced steady flow around the model, after which a second shock was incident on the model. The time between the arrival of the shocks in the working section was 100 μsec. The stream Mach number behind the first shock was M_1 = 1.44-1.50, and of the second shock was M_2 = 1.4-1.5. The density was measured by using a Mach–Zender interferometer whose light source was a Q-modulated ruby laser. The Q-modulation was accomplished by an electrooptical shutter on the basis of a KDP crystal. A typical interferogram is presented in Fig. 1. The bow wave (1), the incident wave (2), and the wave reflected from the body surface (3) are seen. The body diameter d is 10 mm.

As is known, the change in density in an axisymmetric flow can be found from the inverted Abel equation [7]:

$$\Delta\rho(r,\ z) = -\frac{\lambda}{\pi k}\int\limits_{r}^{R(z)} \frac{\partial\delta}{\partial y}(y,\ z)\frac{dy}{\sqrt{y^2-r^2}}\ .$$

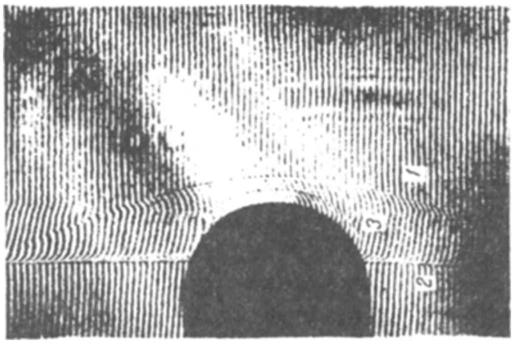

Fig. 1. Typical interferogram. t = 3.4 μsec.

Here $\Delta\rho$(r, z) is the change in density, λ is the laser radiation wavelength, and δ(r, z) is the shift in the interference fringes.

Experimental values of the quantity δ(r, z) were approximated by even power Chebyshev polynomials to determine $\Delta\rho$(r, z).

Density fields near a spherical nose at different times are plotted in Fig. 2. Presented in Fig. 2a and b are the results for two stages of unsteady flow. The time is measured from the time the incident and bow waves meet. Here I is the bow wave, II is the reflected shock, and III is the contact surface which originates when the reflected and bow shocks merge. Shown in Fig. 2c is the density distribution

M. V. Lomonosov Moscow State University. Translated from Inzhenerno-Fizicheskii Zhurnal, Vol. 25, No. 1, pp. 107-110, July, 1973. Original article submitted December 14, 1972.

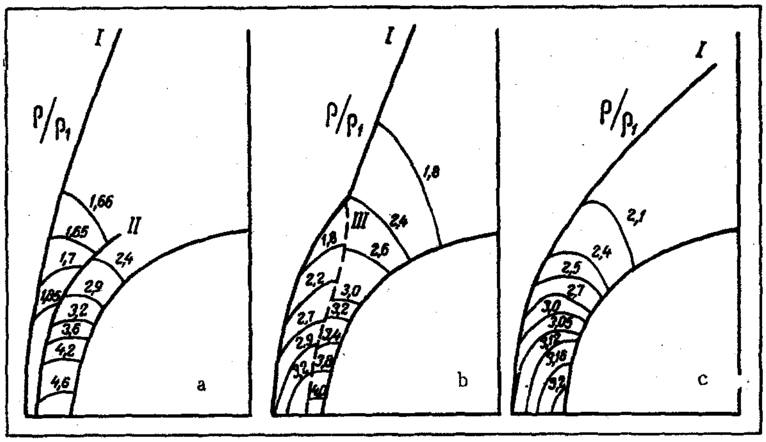

Fig. 2. Density fields near a spherical nose: a) t = 4.5 μsec; b) t = 10 μsec.

for steady flow around the body by the stream behind the second wave. The density in the shock layer is referred to the density ahead of the bow wave. These data show that the distribution of the relative density in the gas layer between the bow and reflected waves is close to the initial value.

Presented in Fig. 3 is the time change in the relative density for three points on the axis of symmetry after incidence of the second shock on a cylinder with a spherical (a) and flat (b) nose: directly behind the bow wave (1), upstream on the contact surface (2), and at the stagnation point (3). The time t_1 corresponds to collision of the transient wave with the body nose; t_2 corresponds to the merging of the reflected and bow waves ahead of the body, and t_3 corresponds to the time when the reflected shock becomes fixed relative to the body. An experimental analysis of the data available in [4-6] as well as the computations [1] show that the pressure at the stagnation point, the bow wave velocity, and the gas velocity on the axis of symmetry reach their steady-state values after the arrival of the rarefaction wave being formed during merger of the bow and reflected waves. The subsequent wave interactions are not shown in the figures and their influence on the mentioned parameters is not essential.

The density at a given point of the perturbed domain can take on the steady value only after the gas particles passing through the bow wave which is fixed relative to the body have arrived at this point. The time interval t_4 between the beginning of wave interaction and the time when the contact surface reaches the body can be taken as the characteristic density build-up time. In our case t_4 = 18 μsec (spherical nose), t_4 = 34 μsec (flat nose) and considerably exceeds the time interval between the beginning of wave interaction and the time when the rarefaction wave reaches the bow wave.

In the tests conducted t_3 was 11 and 16 μsec for the spherical and flat nose, respectively. The diminution in the density at the stagnation point is seen clearly in Fig. 3, which even continues for $t > t_3$, as is also its weaker change directly behind the bow shock. The maximum value of the density at the stagnation point exceeds its stationary value 1.4-fold (spherical nose) and 1.7-fold (flat nose).

NOTATION

r, z are the cylindrical coordinates;
R(z) is the shock radius;
M_1 is the stream Mach number behind the first shock front;
M_2 is the Mach number of the wave incident on the body;

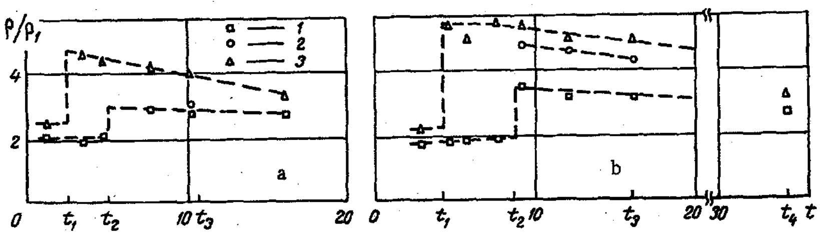

Fig. 3. Time change in the relative density; t in μsec.

ρ is the gas density;
$\Delta\rho$ is the density increment;
ρ_1 is the gas density in the stream behind the shock impinging on the body;
δ is the shift of the interference fringes;
λ is the wavelength of light;
k is the Gladstone–Daley constant;
t_1 is the time interval between the beginning of wave interaction and the collision of the transient wave at the body stagnation point;
t_2 is the time interval between the beginning of wave interaction and the time of reflected wave merger with the bow shock;
t_3 is the time interval after which the reflected shock becomes fixed relative to the body;
t_4 is the time interval between the beginning of wave interaction and the time when the contact surface reaches the body nose;
d is the body diameter (d = 10 mm).

LITERATURE CITED

1. Taylor and Huggins, Raketnaya Tekhn. i Kosmonavtika, 6, No. 2, 8 (1968).
2. W. McNamara, Jnl. Spacecraft and Rockets, 4, No. 6, 790 (1967).
3. V. B. Balakin and V. V. Bulanov, Inzh.-Fizich. Zh., 21, No. 6, 1033 (1971).
4. J. R. Ruetenik and B. Lemcke, Jnl. Spacecraft and Rockets, 4, No. 8, 1030 (1967).
5. A. I. Akimov, Yu. G. Lisin, F. V. Shugaev, and Yu. F. Makovskii, Uchenye Zapiski TsAGI, 2, No. 2, 94 (1971).
6. F. V. Shugaev and Yu. G. Lisin, Inzh.-Fizich, Zh., 21, No. 3, 419 (1971).
7. L. A. Vasil'ev, Shadowgraph Methods [in Russian], Nauka, Moscow (1968).